

$\text{Re } n' \sim \text{Im } n' \sim \beta_e^{-1/2}$  for  $|1 - 2\omega_H^e/\omega| \leq \beta_e^{1/2}$ ,  $|A_0|^3 \leq \beta_e^2$ .

We now consider cases of ion cyclotron resonance. If  $\omega \approx \omega_H^i$ , the indices of refraction for the ordinary and extraordinary waves (when  $\beta_{ic} \ll V_A \ll c$ ) are given by the expressions

$$n_1^2 = N_+^2 = \frac{1 + \cos^2 \theta}{\cos^2 \theta} \frac{c^2/V_A^2}{u_i - 1}, \quad n_2^2 = N_-^2 = \frac{c^2/V_A^2}{1 + \cos^2 \theta}, \quad (2)$$

where  $c^2/V_A^2 = (\Omega_i/\omega_H^i)^2$  (the subscript  $i$  used in the quantity  $f_i$  denotes the quantity  $f_e$  with the electron mass replaced by the ion mass  $m_i$  and the temperature of electron gas replaced by the ion temperature  $T_i$ ). The expression for  $n_1$  given in (2) applies when  $|1 - \omega_H^i/\omega| \gg \beta_{iN_+} \cos \theta$ ; in this case the cyclotron damping of the ordinary wave is exponentially small. When  $|1 - \omega_H^i/\omega| \ll \beta_{iN_+} \cos \theta$  however, this wave is highly damped:

$$n_1' = n_1 + i\alpha_1 = \frac{\sqrt{3} + i}{2} \left\{ \sqrt{\frac{\pi}{8}} \frac{c^2(1 + \cos^2 \theta)}{V_A^2 \beta_i \cos^3 \theta} \right\}^{1/2}. \quad (3)$$

The extraordinary wave also experiences cyclotron absorption:

$$\alpha_2 = \beta_i N_-^2 \cos \theta \sin^4 \theta \exp(-z_1^2) / \sqrt{8\pi} |\omega(z_1^i)|^2 (1 + \cos^2 \theta)^2, \quad (4)$$

where

$$z_1^i = (1 - \omega_H^i/\omega) (\sqrt{2} \beta_i N_- \cos \theta)^{-1},$$

$$\omega(z) = e^{-z^2} \left( 1 + \frac{2i}{\sqrt{\pi}} \int_0^z e^{t^2} dt \right).$$

The extraordinary wave is weakly damped:  $\kappa_2 \ll N_-$  since  $\beta_{iN_-} \ll 1$ . When  $\beta_{ic} \sim V_A$  propagation of both waves is impossible because of the strong damping:  $n_{1,2} \sim \kappa_{1,2} \sim 1/\beta_i$  if  $\omega \sim \omega_H^i$ .

In the case of multiple resonances

$$\omega \approx m\omega_H^i, \quad m = 2, 3, \dots, \quad n_{1,2}' = N_{\pm} + i\alpha_{1,2},$$

where

$$N_{\pm}^2 = \{\varepsilon_{11}(1 + \cos^2 \theta) \mp [\varepsilon_{11}^2(1 + \cos^2 \theta)^2 - 4 \cos^2 \theta (\varepsilon_{11}^2 + \varepsilon_{12}^2)]^{1/2}\} / 2 \cos^2 \theta, \quad (5)$$

$$\alpha_{1,2} = \sigma_m^i N_{\pm} \{ (1 + \cos^2 \theta) N_{\pm}^2 - 2\varepsilon_{11} - 2i\varepsilon_{12} \} \{ 2 \cos^2 \theta N_{\pm}^4 - \varepsilon_{11}(1 + \cos^2 \theta) N_{\pm}^2 \}^{-1}, \quad (6)$$

$$\sigma_m^i = \frac{\sqrt{\pi} m^{2m-2} \sin^{2m-2} \theta c^2}{2^{m+1/2} m! \cos \theta V_A^2} (\beta_i N_{\pm})^{2m-3} \exp(-z_m^i),$$

$$z_m^i = (1 - m\omega_H^i/\omega) (\sqrt{2} \beta_i N_{\pm} \cos \theta)^{-1}, \quad \varepsilon_{11} = 1 - v_i/(1 - u_i),$$

$$\varepsilon_{12} = -iv_i/\sqrt{u_i}(1 - u_i).$$

If  $|z_m^i| \lesssim 1$ , then  $\kappa_{1,2}/N_{\pm} \sim (\beta_i N_{\pm})^{2m-3}$ .

Waves characterized by frequencies  $\omega \sim \omega_H^i$

( $\omega$  not necessarily close to  $m\omega_H^i$ ) are also damped as a consequence of absorption in the electron gas (Landau damping). The refractive indices for these waves are given by Eq. (5) and the damping coefficients are

$$\alpha_{2,3}/N_{\pm} = \text{Im} \left\{ \frac{1}{\varepsilon_{33}} [\varepsilon_{11} \sin^2 \theta N_{\pm}^4 + (2\varepsilon_{12}\varepsilon_{23} \cos \theta \sin \theta - \varepsilon_{23}^2 \cos^2 \theta - (\varepsilon_{11}^2 + \varepsilon_{12}^2) \sin^2 \theta) N_{\pm}^2 + \varepsilon_{11}\varepsilon_{23}^2] + \varepsilon_{22} (\varepsilon_{11} - \cos^2 \theta N_{\pm}^2) \right\} \times \{ 2\varepsilon_{11}(1 + \cos^2 \theta) N_{\pm}^2 - 4 \cos^2 \theta N_{\pm}^4 \}^{-1}, \quad (7)$$

where

$$\varepsilon_{23} = -i \tan \theta v_i (1 + i\sqrt{\pi} z_0^e \omega(z_0^e)) / \sqrt{u_i},$$

$$\varepsilon_{22} = i 2\sqrt{\pi} (m_e/m_i) \sin^2 \theta v_i z_0^e \omega(z_0^e) \beta_e^2 N_{\pm}^2 / u_i,$$

$$\varepsilon_{33} = (2m_i/m_e) v_i (z_0^e)^2 (1 + i\sqrt{\pi} z_0^e \omega(z_0^e)),$$

$$z_0^e = (\sqrt{2} \beta_e N_{\pm} \cos \theta)^{-1}.$$

The damping (7) is small;  $\kappa_{2,3} \ll N_{\pm}$ . Even if  $|z_0^e| \lesssim 1$ , i.e.,  $V_A \sim \beta_e c$ , we find  $\kappa_{2,3}/N_{\pm} \sim m_e/m_i$ .

<sup>1</sup>V. P. Silin, Тр. ФИАИ СССР (Proc. Inst. Phys. Acad. Sci. U.S.S.R.) **6**, 199 (1955).

<sup>2</sup>A. G. Sitenko and K. N. Stepanov, JETP **31**, 642 (1956), Soviet Phys. JETP **4**, 512 (1957).

<sup>3</sup>K. N. Stepanov, JETP **35**, 283 (1958), Soviet Phys. JETP **8**, 195 (1959).

<sup>4</sup>R. Z. Sagdeev and V. D. Shafranov, (Proceedings of the Second International Conference on the Peaceful Uses of Atomic Energy) Vol. I, Moscow, 1959, p. 202.

<sup>5</sup>V. D. Shafranov, Физика плазмы и проблема управляемых термоядерных реакций (Plasma Physics and the Problem of a Controlled Thermonuclear Reaction), Acad. Sci. U.S.S.R., 1958, Vol. IV, p. 426.

<sup>6</sup>V. N. Gershman, JETP **24**, 659 (1953).

Translated by H. Lashinsky

51

## CURVES FOR THE PHOTOPROTON YIELD FROM THE $C^{12}$ NUCLEUS

E. B. BAZHANOV

Leningrad Physico-technical Institute, Academy of Sciences, U.S.S.R.

Submitted to JETP editor August 14, 1959

J. Exptl. Theoret. Phys. (U.S.S.R.) **38**, 267-269 (January, 1960)

A previously described<sup>1</sup> scintillation telescope was used to investigate the dependence of the photo-

proton yield from the  $C^{12}$  nucleus on the peak energy of bremsstrahlung  $\gamma$  rays. Yield curves were simultaneously obtained for three proton energy intervals: 18.6–24.2 Mev, 24.2–29.9 Mev, and 29.9–38.7 Mev with average energies of 21.4, 27.0, and 34.3 Mev respectively. All the measurements were made with an angle  $\theta = 57.5^\circ$  with respect to the direction of the  $\gamma$  beam, and the maximum angular resolution of the telescope was  $\pm 6.0^\circ$ . The target, 150 mg/cm<sup>2</sup> thick, was placed perpendicular to the beam. The absolute doses of the  $\gamma$  rays that had passed through the target for each peak  $\gamma$  energy were measured with a thick-walled copper ionization chamber, which had been calibrated with a calorimeter.<sup>2</sup> The sensitivity of the ionization chamber to bremsstrahlung  $\gamma$  rays was practically independent of the peak  $\gamma$  energy within the energy interval used.

Figures 1, 2, and 3 present the experimental results for the average proton energies given above. Smooth curves (labeled a) were plotted through the experimental points, and after a preliminary procedure to smooth out the original variations, the Penfold-Leiss<sup>3</sup> method was used to convert them into cross section curves (labeled b). The statistical accuracy of the experiment was insufficient to prove the existence of a second maximum in the cross section curve in Fig. 1. However, since the yield curve is seen to rise generally right up to the largest energies, it appears altogether probable that there is a long "tail" like the one indicated in Fig. 3. The curves labeled c represent Dedrick's calculations<sup>4</sup> based on a quasi-

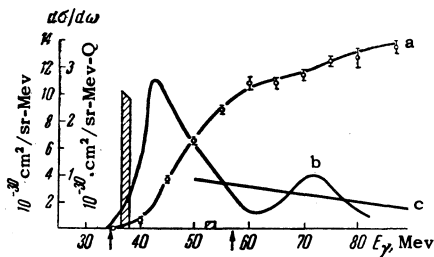


FIG. 1. Photoproton yield and cross section curves for  $C^{12}$  with  $\bar{E}_p = 21.4$  Mev. The right ordinate scale refers to curve a and the left to curves b and c and the shaded areas. The errors are statistical.

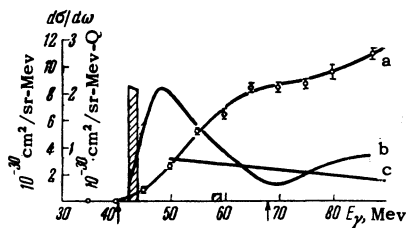


FIG. 2. The same as in Fig. 1, but for photoprotons with  $\bar{E}_p = 27.0$  Mev.

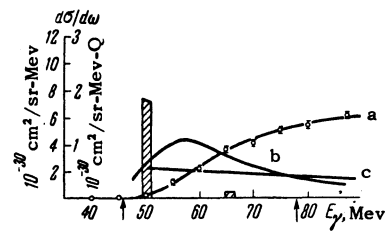


FIG. 3. The same as in Fig. 1, but for photoprotons with  $\bar{E}_p = 34.3$  Mev.

deuteron mechanism of  $\gamma$ -nucleus interaction. It must be noted that agreement with the experiment for high energies is entirely satisfactory. Similar agreement has been observed<sup>5</sup> in the case of photoprotons with an average energy of 37 Mev. The arrows to the right along the abscissa indicate the minimum  $\gamma$  energies necessary for the formation of protons with a minimum energy for the corresponding interval. These energies were obtained from the known kinematical relation, which is based on the conservation laws for the interaction between  $\gamma$  quanta and a quasi-deuteron in the nucleus:

$$E_\gamma = \frac{2E_p}{1 - E'_p/M + p' \cos \theta / M},$$

$$E_p = E_{p \min} + \frac{1}{2} E_{\text{binding}}(\gamma, pn).$$

In our opinion the wide maximum observed in the case of comparatively low  $\gamma$  energies is to a considerable extent due to a contribution by the  $C^{12}(\gamma p)B^{11}$  reaction. In favor of this view is the good correspondence which exists between the experimental thresholds for the reaction and those predicted on the basis of the relation

$$E_{\gamma \min} = E_{p \min} + E_{\text{binding}}(\gamma p),$$

where  $E_{\text{binding}}(\gamma p) = 16$  Mev (the arrows to the left). Shklyarevskii<sup>6</sup> has used the harmonic oscillator potential to investigate the interaction of  $\gamma$  quanta with any individual nucleon in a nucleus or with the remaining non-participating nucleons on the basis of an independent particle model. The shaded areas in the figures represent the contribution by  $(1p)^4$  and  $(1s)^2$  shells as determined by Shklyarevskii's formulae. The parameter  $\epsilon = \hbar\omega_0$ , which represents the separation between the shells, is assumed to be equal to 15.5 Mev on the basis of Hofstadter's data.<sup>7</sup> The dependence of the well depth,  $V_0$ , on the proton energy<sup>8</sup> was also taken into consideration. The effective well depth was computed from the following relation:

$$V_{\text{eff}}^l = V_0(E_p) - \bar{V}^l, \quad \bar{V}^l = \int_0^\infty \varphi_{nlm}^*(r) V(r) \varphi_{nlm}(r) dr,$$

where  $\varphi_{nlm}(r)$  is the oscillator wave function. When  $l = 0$ ,  $\bar{V}^0 = 3/4 \epsilon$ ; when  $l = 1$ ,  $\bar{V}^1 = 5/4 \epsilon$ . The

contribution from the  $(1s)^2$  shell does not exceed 6% of the contribution from the  $(1p)^4$  shell in all cases.

Shown below for comparison are the integral cross sections computed with the Shklyarevskii formulae and those obtained experimentally:

Interval of proton energy, Mev	18.6–24.2	24.2–29.9
Integration interval of experimental data, Mev	34–63	42–70
Integral cross section obtained experimentally, $10^{-30}$ cm <sup>2</sup> Mev/sr	$135.2 \pm 20.6$	$120.6 \pm 18.9$
Computed integral cross section, $10^{-30}$ cm <sup>2</sup> Mev/sr	10.5	8.8

The difference by a factor of ten should be considered too large, even making allowances for the approximate nature of the theoretical computations, as well as for the fact that a quasi-deuteron interaction mechanism may also introduce a certain contribution to the experimental integral cross section. The 5–7 Mev shift toward high  $\gamma$  energies of the experimental maximum that can be seen in all the graphs relative to the computed contribution from the  $(1p)^4$  shell can be explained by the fact that all of Shklyarevskii's calculations are based on the assumption that the final nucleus remains in the ground state, which, of course, is hardly probable.

The author wishes to thank Prof. A. P. Komar and his laboratory associates for their interest in this paper and also L. E. Lazarev for kindly making possible the use of the tables<sup>3</sup> for computing the cross section curves.

<sup>1</sup>Bazhanov, Volkov, and Kul'chitskii, JETP **35**, 322 (1958), Soviet Phys. JETP **8**, 224 (1958).

<sup>2</sup>S. P. Kruglov, J. Tech. Phys. (U.S.S.R.) **28**, 2310 (1958), Soviet Phys.-Tech. Phys. **3**, 2120 (1958).

<sup>3</sup>A. S. Penfold and J. E. Leiss, Analysis of Photo Cross Sections, University of Illinois (1958).

<sup>4</sup>K. G. Dedrick, Phys. Rev. **100**, 58 (1955).

<sup>5</sup>Whitehead, McMurray, Aitken, Middlemas, and Collie, Phys. Rev. **110**, 941 (1958).

<sup>6</sup>G. M. Shklyarevskii, JETP **36**, 1492 (1959), Soviet Phys. JETP **9**, 1057 (1959).

<sup>7</sup>R. Hofstadter, Ann. Rev. Nuclear Sci. **7**, 231 (1957).

<sup>8</sup>A. E. Glassgold, Revs. Modern Phys. **30**, 419 (1958).

## MAGNETIC ANISOTROPY OF THE DISORDERED ALLOY Ni<sub>3</sub>Mn AT HELIUM TEMPERATURES

N. V. VOLKENSHTEĪN and M. I. TURCHINSKAYA

The Metal Physics Institute, Academy of Sciences, U.S.S.R.

Submitted to JETP editor August 28, 1959

J. Exptl. Theoret. Phys. (U.S.S.R.) **38**, 270–271 (January, 1960)

FOR polycrystalline specimens of the alloy Ni<sub>3</sub>Mn in the disordered state, a number of workers<sup>1–3</sup> have shown that the reversible magnetization curves taken at liquid helium temperatures lie significantly below the curves taken at liquid hydrogen temperature and do not attain saturation at tens of thousands of oersteds. Magnetization curves of this type could be due to a rapid temperature variation of the magnetic anisotropy. To resolve this question a study is required on single crystals — the magnetization curves being taken in various crystallographic directions. We have performed such a study.

From a large single crystal of the alloy Ni<sub>3</sub>Mn with face-centered cubic lattice in the disordered state, specimens of prismatic shape ( $1.2 \times 1.2 \times 18$  mm<sup>3</sup>) were cut, the long axes of which were parallel respectively to the three crystallographic directions: [111], [110], [100]. The reversible magnetization curves of these specimens were taken at room temperature and at liquid nitrogen, hydrogen, and helium temperatures.

The results are given in the figure. From the curves it is seen that at room temperature for all crystallographic directions there is a linear dependence of induction on field, and there is no anisotropy.

On going to nitrogen temperature the character of the curves undergoes a marked change. Firstly, the curves  $4\pi I(H)$  assume a form typical of a ferromagnet. Secondly, magnetic anisotropy appears; it increases on lowering the temperature to liquid-hydrogen temperature, but does not change essentially on further cooling to liquid-helium temperature. The crystallographic direction [100] remains the difficult, [111] the easy, and [110] the intermediate direction throughout the temperature interval studied (from 77.8 to 4.2°K). In spite of the fact that the magnetic anisotropy (a measure of which is the area included between the curves for the [100] and [111] axes) does not in-